Received: 4 May 2023 | Revised: 5 December 2023 | Accepted: 13 January 2024

DOI: 10.1002/est2.588

RESEARCH ARTICLE

ENERGY STORAGE WILEY

Battery degradation: Impact on economic dispatch

Curd Schade[1,2] | **Ruud Egging-Bratseth**[1]

[1]Department of Industrial Economics and Technology Management, Norwegian University of Science and Technology, Trondheim, Norway

[2]Workgroup for Infrastructure Policy, Technical University Berlin, Berlin, Germany

Correspondence
Ruud Egging-Bratseth, Department of Industrial Economics and Technology Management, Norwegian University of Science and Technology, Trondheim, Trøndelag, 7491, Norway.
Email: ruude@ntnu.no

Abstract

Batteries are crucial to manage the rising share of intermittent energy sources and variability in demand. Most technoeconomic models in the literature oversimplify battery degradation representation. Accounting properly for battery degradation allows for better cost tradeoffs and optimal battery usage, especially in dynamic settings. We propose a highly accurate and scalable formulation for battery degradation that considers the combined impact of cycle depth (CD) and state of charge on calendar and cycle aging. This includes a novel way to track charge-discharge cycles. We test the consequences of battery degradation in a stylized price arbitrage model on battery operation and solution times. When ignoring battery degradation, ex post calculations reveal hidden degradation costs that exceed revenues and hence turn seemingly profitable trades into losing trades. Considering battery degradation leads to smaller CDs and lower average states of charge. Overall, we show that a much-improved representation of battery degradation is possible at modest computational cost, allowing better decisions and higher profits.

KEYWORDS

battery degradation, calendar aging, cycle depth, economic dispatch, state of charge

1 | INTRODUCTION

Batteries have favorable characteristics such as high power and energy density, flexibility in spatial placement and sizing, and fast response times. These characteristics allow a multitude of applications ranging from economic energy arbitrage to systemic benefits like voltage regulation and optimal renewable energy allocation.[1-3] Intensive use of batteries accelerates their aging due to physical and chemical stresses, leading to reduced performance and reduced safety.[4,5] Batteries are expensive, and their degradation should be minimized to maximize their lifetime. However, in settings with very high and low electricity prices, minimizing battery degradation may mean charging or discharging at unfavorable prices and forgoing opportunities to charge very cheaply. Arbitraging price differences can allow for steep financial gains; however, at the expense of increased battery degradation. Models for smart grids and other dispatch models should explicitly trade off profit opportunities with the added battery stress and battery life reduction.

This paper addresses two questions: *How do different battery degradation mechanisms affect battery operation in an economic dispatch setting?*, and *How can we balance accurate battery degradation formulations with model scalability?*

In the following, we discuss battery structure and aging mechanisms, and their relevance in economic dispatch modeling. We formulate an economic dispatch model for price arbitrage with adequate, scalable

functional forms for three main battery degradation mechanisms: Cycle Depth (CD), average cycle state of charge (SOC), and SOC-based calendar aging. We also contribute a new cycle counting formulation, and perform a sensitivity analysis on battery replacement costs.

We assess the impact of the degradation on optimal battery dispatch, capturing over 95% of battery degradation and solution times short enough for practical applications.

2 | LITERATURE

Lithium-ion batteries consist of a carbonaceous anode, a metal oxide cathode, a lithium salt electrolyte, and a separator. Each of these four components experiences degradation, causing decreasing power output and reducing the maximum stored energy, thus affecting overall battery lifetime. Battery lifetime is related to a battery's purpose. Typically, end of life means that the battery's capacity is reduced so much that it can no longer adequately perform its intended purposes.

Battery life has two components: calendar life, and cycle life, which are additive, so we minimize both.[6,7] Calendar life corresponds to the time before the battery reaches a purpose-specific capacity threshold (eg, for electric vehicles [EVs] this is often considered to be 80%). Cycle life is connected to the number of charge and discharge cycles a battery can experience before the battery reaches its end of life. In frequently used batteries, the cycle life is the decisive component of lifetime.[8] Stationary, grid-connected, batteries are often used frequently; hence, for these, cycle life tends to be decisive for their life. In contrast, EV batteries are typically idle most of the time, with few charge cycles. For EVs calendar aging is very often the main factor impacting battery life.

2.1 | Calendar degradation mechanisms

Calendar aging is mostly driven by time, ambient temperature, and the SOC. Time, and, often, ambient temperature, are uncontrollable, external parameters, while the SOC is affected by operational decisions.[8-10] Prolonged, high SOC levels are devastating to batteries.[9,11]

Most batteries operate optimally at a cell temperature of approximately 25°C.[4] While cell temperature has a very significant impact, with about doubled battery aging for every 10°C to 15°C increase, it is an easily controllable parameter in stationary conditions. Furthermore, it is difficult to assess the influence of the ambient temperature on cell temperature, especially for actively used batteries in low ambient temperature conditions. Therefore, temperature is often not considered in (technoeconomic) optimization models.[5,12-14] Finally, while low ambient temperatures are beneficial for the calendar lifetime, they can be harmful to the cycle lifetime.[15]

2.2 | Cycle degradation mechanisms

Besides the intended exchange of electrons, battery charging and discharging causes side reactions that promote battery degradation by increasing the internal resistance and reducing the storage capacity. Physical aging refers to the loss of active material (eg, lithium oxide) in the electrodes, and is affected by operating decisions CD and SOC. In contrast, chemical aging refers to the loss of material for transport between electrodes (eg, lithium inventory), and is affected by calendar time, cell temperatures, and current rate (C-rate) when charging and discharging.[4,8]

Battery cycling induces physical stresses in the form of volume changes through the intercalation and deintercalation of lithium ions in the anode and the cathode. These volume changes lead to particle fractures at the electrodes, thereby exposing additional electrode surface to the electrolyte, which leads to a growth of the solid-electrolyte interphase (SEI) layer. This in turn results in a permanent drop in cell capacity and thus overall battery capacity.[11]

The four main cycling-related degradation drivers are: CD, C-rate, temperature, and SOC.

Deeper discharge cycles result in faster battery aging.[10,16] In the literature, depth of discharge (DOD) is used for both the absolute discharge level of the battery (such that SOC + DOD = 100%), and for the depth of a discharge compared to a starting SOC that may be different from 100%. We rather use CD for the latter meaning.

Operating a battery with 10% CD compared to 100% CD allows 100 times more cycles and 10 times larger total energy throughput.[17] The pronounced nonlinear relation between CD and aging of Li-ion batteries is typically not accounted for in economic dispatch models.

The second important cycling-related aging driver is the C-rate. It is defined as the (dis)charging current divided by the rated battery storage capacity. Lower C-rates tends to result in lower battery aging.[6] In grid applications, the (dis)charge voltage is considered constant; hence, we express the C-rate relative to a full (dis)charge in 1 h.[2]

Batteries have three degradation phases. A new battery experiences rapid aging due to the initial formation of the SEI layer, resulting in up to 5% capacity loss. In the second phase, the battery is more stable and ages at a slower rate than in the other phases. Batteries spend most

cycles in this stage. After approximately 12% capacity loss (including phase 1) phase 3 follows with accelerated degradation.[5]

While low C-rate are generally good for battery longevity, in low-temperature conditions the discharge efficiency is worse with low discharge rates. This is due to a lower solid-state diffusivity of the Li ions, low ionic conductivity of the electrolyte and much higher interfacial charge transfer resistance.[18]

Regardless of the battery type, C-rates below 1C have modest impact on battery capacity,[8,19] for lithium iron phosphate (LFP) batteries this continues even up to 4C. For EVs battery management systems prevent the occurrence of damaging high C-rates.[20] For batteries in grid applications, the power ratings are usually lower than the energy rating, which prevents C-rates >1C from happening. Consequently, degradation due to C-rate can often be ignored, except in high-power applications such as frequency regulation.[2]

The third important cycling-related aging driver is cell temperature. High cell temperatures accelerate chemical reactions and thus harmful side reactions. Compared to the ambient temperature, the temperature gradient in the battery depends primarily on the C-rate: high C-rate will result in a high cell temperature. It is difficult to separate cell temperature impact from the C-rate stress, and at room temperature the C-rate is the main driver, therefore cell temperature effects can be captured by a C-rate degradation mechanism.

The fourth driver, SOC, is often considered for calendar aging, but it affects cycle aging too. The optimal average SOC for battery cycling is 50%: cycles passing symmetrically through SOC = 50% cause the least damage.[16,21]

3 | BATTERY DEGRADATION

Battery degradation mechanisms have complex nonconvex behavior. This complexity makes integrating battery degradation in economic dispatch models difficult because of numerical tractability. Electrochemical models are the most accurate, but are highly nonconvex and need much data.[22] They do not scale to the longer time horizons considered in economic dispatch models. Many technoeconomic studies consider battery degradation only through fixed upper and lower bounds for SOC and a limit on C-rate.[23,24] From a financial-economic perspective such limits unnecessarily disallow potentially profitable operations. Ignoring other degradation mechanisms, typically leads to high resting SOC level and deep cycles, which are both harmful to battery life.[25] We desire a degradation model usable in economic dispatch optimization that considers factors affected by operational decisions SOC, CD, and C-rate. Hence, we formulate degradation based on measurements of a specific battery cell.[21,26] Total battery degradation equals the sum of calendar and cycle aging[8,27]: $Q = Q^{\mathrm{CAL}} + Q^{\mathrm{CD}}$.

3.1 | Calendar degradation

Arrhenius law is the basis for electrochemical calendar aging models, wherein temperature is the main driver.[28] As we lack data to apply Arrhenius law and rather avoid representing temperature, we opt for an empirically based expression wherein calendar aging increases when longer time is spent at high SOC levels. Several polynomial curve fits have been used to define this aging relationship for battery types LFP[28] and nickel managanese cobalt (NMC).[29] Linear fits are imprecise as they disregard aging plateaus.[7] Higher order polynomial functions are more accurate, and these can be represented using piecewise linear functions.

3.2 | Cycle degradation

To represent CD-induced degradation the rainflow algorithm is commonly used to count the occurring cycles. The nonlinear nature of the algorithm requires either a preprocessing strategy[30] or a widely used piecewise linear approach in the modeling.[9,31-36] The latter allows the penalization of discharges more than proportional to the CD. The basis is the material stress function, which determines capacity loss per cycle as a function of the CD. Two approaches to this stress function exist. First, it can be based on the Arrhenius equation, but this results, however, in a concave stress function,[32] so we disregard this option. Second, it can be based on an amplitude function for physical stress (eg, Equation 1).[9,16] Parameter a displays the maximum capacity loss per cycle, while m is the fatigue strength exponent.

$$Q^{\mathrm{CD}}(\mathrm{CD}) = a^{\mathrm{CD}} \times \mathrm{CD}^{\frac{1}{m}}. \tag{1}$$

This stress function is the input for the segmented cost function Equation (2), wherein r is the battery replacement cost (€/kWh), e^{RAT} battery capacity, and N the number of virtual battery segments.[9] Since it more easily allows implementation of other aging mechanisms compared to other alternatives in the literature, we base Equation (2) for CD-based damage in *virtual segment j* on[33,34]:

$$e^{\mathrm{RAT}} \times r \times \left[Q^{\mathrm{CD}}\left(\frac{j}{N}\right) - Q^{\mathrm{CD}}\left(\frac{j-1}{N}\right)\right]. \quad (2)$$

Naturally, there is a tradeoff in the number and sizes of the segments, and thereby the accuracy of a piecewise linear approximation and the complexity of the resulting model. For the battery type used in our case study, with 16 segments the relative error is approximately 2% only for an NMC battery cell.[9] We try to minimize this error further by considering a nonuniform segmentation in Section 5.2.

4 | MODEL FORMULATION

The model is set up to determine the maximum profit obtainable from charging and discharging the battery, given hourly varying prices, while considering battery degradation costs. We list variable names in Table 1. Parameter values related to the battery can be found in Tables 2 and 3 in Section 5. For reference, we provide sets, variables and parameter names in Tables 6-8 in Nomenclature at the end of the paper.

Equation (3) minimizes the battery degradation cost K over all time steps. We treat the arbitrage profit from charges $C_{j,h}$ (purchases) and discharges $D_{j,h}$ (sales) as negative costs, both multiplied by the hourly electricity price, parameter p_h.

$$\mathrm{MIN}: \sum_h \left(K_h - \left(p_h \times \sum_j \left(D_{j,h} - C_{j,h} \right) \right) \right). \quad (3)$$

We include constraints for operation and for degradation.

4.1 | Battery operation constraints

As indicated previously, we propose a nonuniform virtual battery segmentation. Equation (4) computes the storage level in a segment at the start of a time step as the previous storage level modified by loss-corrected charges or discharges in the previous time step. Equation (5) restricts stored energy in each segment. Equations (6) and (7) restrict charges and discharges to their maximum values.

$$S_{j,h} = S_{j,h-1} + v^C \times C_{j,h-1} - \frac{D_{j,h-1}}{v^D} \ \forall j,h, \quad (4)$$

TABLE 1 Variable names.

Variable	Description
A_h^{CYC}	Deviation from 50% SOC
B_h^{C}	Binary for charging mode
B_h^{D}	Binary for discharging mode
B_h^{END}	Binary for end point of a charging cycle
B_h^{S}	Binary for stationary mode
B_h^{ST}	Binary for starting point of a charging cycle
$C_{j,h}$	Charge volume
$D_{j,h}$	Discharge volume
K_h	Hourly battery degradation costs
Q^{CD}	CD degradation function
Q_h^{CD}	Degradation due to cycle depth
Q_h^{SOC}	Degradation due to average cycling SOC
Q_h^{CAL}	Calendar based degradation due to SOC levels
$S_{j,h}$	Storage level
Q_h^{SOC}	SOC level at the end of hour

Note: Subscripts j and h in various variables indicate *virtual battery segment* and *hour*, respectively.

TABLE 2 Battery input parameters.

Par.	Description	Value(s) (unit)
a	Maximum capacity loss per cycle	0.04519%/cycle
c^{MAX}	Rated (charge) power	60 kW
d^{MAX}	Rated (discharge) power	60 kW
e^{RAT}	Rated energy	100 kWh
f	Fitting parameter SOC stress	0.0085%/cycle
m	Fatigue strength exponent	0.4926
o_j^{CAL}	Calendar aging breakpoint value	In table
o_j^{CD}	SOC breakpoint value	In table
r	Replacement cost	150 €/kWh
v^{C}	Charge efficiency	95%
v^{D}	Discharge efficiency	95%
y_j	Calendar aging breakpoint value	In table

$$S_{j,h} \le e^{\mathrm{RAT}} \times \left(o_{j+1}^{\mathrm{CD}} - o_j^{\mathrm{CD}} \right) \ \forall j,h, \quad (5)$$

$$\sum_j C_{j,h} \le c^{\mathrm{MAX}} \times B_h^{\mathrm{C}} \ \ \forall j,h, \quad (6)$$

$$\sum_j D_{j,h} \le d^{\mathrm{MAX}} \times B_h^{\mathrm{D}} \ \ \forall j,h, \quad (7)$$

TABLE 3 Break point calendar aging values (10^{-7}).

Parameter	Values				
o_j^{CAL}	0%	30%	60%	70%	100%
y_j	3.75	8.76	10.01	18.41	22.34

$$B_h^S \geq 1 - \sum_j \left(D_{j,h} + C_{j,h}\right) \quad \forall j,h, \tag{8}$$

$$B_h^C + B_h^D + B_h^S = 1 \quad \forall h. \tag{9}$$

Equations (8) and (9) compute binary variables for the mutually exclusive battery modes charging, discharging and steady state, which are used to count cycles and determine battery degradation. The reader may notice that Equation (8) enforces a minimum charge or discharge of 1. The scaling of the data is such that this is never binding. It is computationally cheaper to use continues variables in the right-hand side of Equation (8), however, a more general formulation would use a bigM.

4.2 | Battery degradation constraints

We adopt the widely used rainflow algorithm-based model for CD. In addition, we consider the influence of the SOC on both calendar and cycle aging. Thus, the model considers three aging factors: CD, average cycling SOC and SOC-based calendar aging.

The degradation costs K consist of the sum of three individual capacity losses Q (%) multiplied by the replacement cost r in €/kWh and e^{RAT} in kWh.

$$K_h = r \times e^{RAT} \times \left(Q_h^{CD} + Q_h^{SOC} + Q_h^{CAL}\right) \quad \forall h. \tag{10}$$

4.2.1 | CD-based degradation

To reflect the nonuniform virtual segmentation for the Q^{CD}, in Equation (11) we multiply the rated energy e^{RAT} with the length of each segment. Here, o_j^{CD} is the SOC value at the segment breakpoint.

To measure CD degradation, we keep track of accumulative discharges in consecutive time periods, not interrupted by periods with charges or without activity. Equation (11) computes the (accumulative) CD-based capacity loss after each discharging time period. To do so, the first term locates all segments that the discharge in the current time step passes through and how much of each segment is discharged. The second term is the degradation value of specific segments computed with piecewise linear function $Q^{CD}(\cdot)$.

$$\forall h,j : Q_h^{CD} = \sum_j \left(\frac{D_{j,h}}{e^{RAT} \times \left(o_{j+1}^{CD} - o_j^{CD}\right)} \times \left[Q^{CD}\left(o_{j+1}^{CD}\right) - Q^{CD}\left(o_j^{CD}\right) \right] \right). \tag{11}$$

4.2.2 | Average cycle SOC degradation

We introduce auxiliary variables to track battery cycles and SOC levels to compute the average cycle SOC degradation at the end of each discharge cycle. First, Equation (12) computes the SOC at the end of every hour.

$$SOC_h = \frac{\sum_j S_{j,h}}{e^{RAT}} \forall h. \tag{12}$$

Equations (13)-(15) and Equations (16)-(18) compute start and end points of individual discharging cycles respectively.

$$B_h^{ST} \geq B_h^D - B_{h-1}^D \quad \forall h, \tag{13}$$

$$B_h^{ST} \leq 1 - B_{h-1}^D \quad \forall h, \tag{14}$$

$$B_h^{ST} \leq B_h^D \quad \forall h, \tag{15}$$

$$B_h^{END} \geq B_{h-1}^D - B_h^D \quad \forall h, \tag{16}$$

$$B_h^{END} \leq B_{h-1}^D \quad \forall h, \tag{17}$$

$$B_h^{END} \leq 1 - B_h^D \quad \forall h. \tag{18}$$

Equation (19) uses B_h^{ST} to save the SOC at the start of a cycle in auxiliary variable A_h^{ST}. In the following timesteps, as long as the cycle continues, the first term becomes zero and the second term copies the value of the previous timestep. One time step after the cycle end, A^{ST} becomes zero due to B_{h-1}^{END}.

$$A_h^{ST} = SOC_h \times B_h^{ST} + \left(1 - B_h^{ST} - B_{h-1}^{END}\right) \times A_{h-1}^{ST} \quad \forall h. \tag{19}$$

Equations (20) and (21) compute the deviation between the average SOC and 50%.

$$A_h^{\mathrm{CYC}} \geq \frac{\mathrm{SOC}_h + A_h^{\mathrm{ST}}}{2} - \frac{1}{2} \quad \forall h, \tag{20}$$

$$A_h^{\mathrm{CYC}} \geq \frac{1}{2} - \frac{\mathrm{SOC}_h + A_h^{\mathrm{ST}}}{2} \quad \forall h. \tag{21}$$

Finally, Equation (22) computes the cycle degradation, at the end of each cycle.

$$Q_h^{\mathrm{SOC}} = f \times A_h^{\mathrm{CYC}} \times B_h^{\mathrm{END}} \quad \forall h. \tag{22}$$

Note that Equations (19) and (22) are bilinear constraints. The Gurobi solver can handle such constraints efficiently.

4.2.3 | Calendar degradation

To calculate the calendar life loss Q^{CAL} we use SOS2 variables via Equations (23)-(25). Equation (26) selects the appropriate segment and computes weighting factors $Z_{i,h}$. Equation (27) determines the calendar aging.

$$\sum_i Z_{i,h} = 1 \quad \forall i,h, \tag{23}$$

$$B_{h,i}^{\mathrm{CAL}} + B_{h,i'}^{\mathrm{CAL}} \leq 1 \quad \forall i, i' > i+1, h, \tag{24}$$

$$Z_{i,h} \leq B_{i,h}^{\mathrm{CAL}} \quad \forall i,h, \tag{25}$$

$$\mathrm{SOC}_h = \sum_i \left(o_i^{\mathrm{CAL}} \times Z_{i,h}\right) \quad \forall i,h, \tag{26}$$

$$Q_h^{\mathrm{CAL}} = \sum_i \left(y_i \times Z_{i,h}\right) \quad \forall i,h. \tag{27}$$

5 | CASE STUDY

We apply our model to assess the impact of the three considered degradation mechanisms and conduct a sensitivity analysis on battery replacement costs. The optimization is implemented in Pyomo, using Gurobi solver 9.1.2 on an Intel Core i5-6200U CPU @ 2.30 GHz, 8 GB RAM. Solution times for specific instances vary from a few seconds to about an hour.

5.1 | Input parameters

The data that support the findings of this study are openly available in *Zenodo* at https://zenodo.org/doi/10.5281/zenodo.10255080.[37] We consider a 2-day period, 22 to 24 April 2019 with hourly German spot prices,[38] to which we add a grid fee of 7.39 ct[39] and 19% value-added tax. Any negative hourly prices based on this are replaced by the value 0.1 ct/kWh. We fix the start and end SOC level to zero. We consider an NMC battery, values ares given in Table 2. The maximum C-rate, or power to energy ratio, is 0.6. Values for a, m, f are estimated based on Laresgoiti et al[16] (c.f. Figure 1).

In contrast to Laresgoiti et al,[16] we disregard the positive constant (the function value at 50% SOC) for parameter f as it is CD damage and we reflect that mechanisms separately. Also, we scale the value by the maximum deviation of 50%.

For the calendar degradation, we compute hourly degradation values from the 10-month NMC data at 25°C from the piecewise linear curves with plateaus in the study of Keil et al.[7] As several studies give significantly lower annual calendar degradation values at full SOC than 8%, we divide the values by 4. Accordingly, a permanent 100% SOC then causes 2% capacity loss per year. Table 3 shows the five chosen breakpoints, and Figure 2 presents the piecewise linear function.

We parameterize the model with values for hourly prices and battery degradation mechanisms. We perform several analyses to validate the model and to analyze the impacts of different types of battery degradation on battery charging and discharging behavior, and profitability of price arbitrage.

5.2 | Model calibration and validation

We verify model outcomes for degradation with this formula: Relative error = (model value/measured value) − 1, wherein *measured value* may be an interpolation between two actual measurement points from a literature source. For convex functions, piecewise linear segments are always above the curve, and Relative error ≥0.

First, we compare a uniform segmentation and a nonuniform segmentation optimized for minimal average distance between segments and the original curve (c.f. Imamoto and Tang[40]). The segment breakpoint locations turn out to be very similar. In the nonuniform approach, the breakpoints shift somewhat toward the steeper upper end of the stress function, making that part more accurate, and the lower segments are larger and slightly less accurate. We perform a model run considering Q^{CD} only, and find that the battery cycles most often in the lower segments, which are better represented in the uniform segmentation. The nonuniform segmentation performs slightly worse. However, the difference in relative error is small: 5.000% for uniform segmentation and 5.007% for the nonuniform. We continue the analyses using a uniform segmentation.

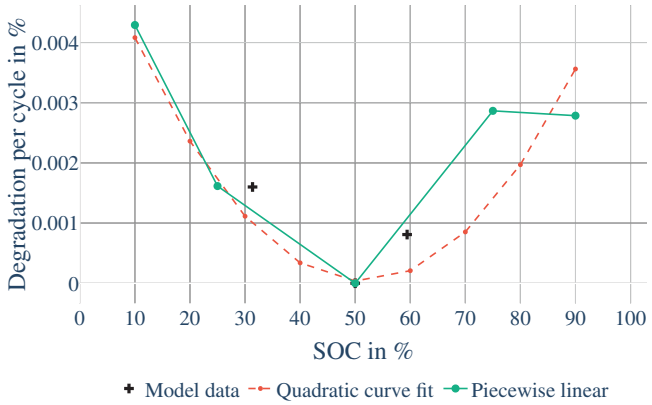

FIGURE 1 Data points, piecewise linear and quadratic curve fit for cycle aging.

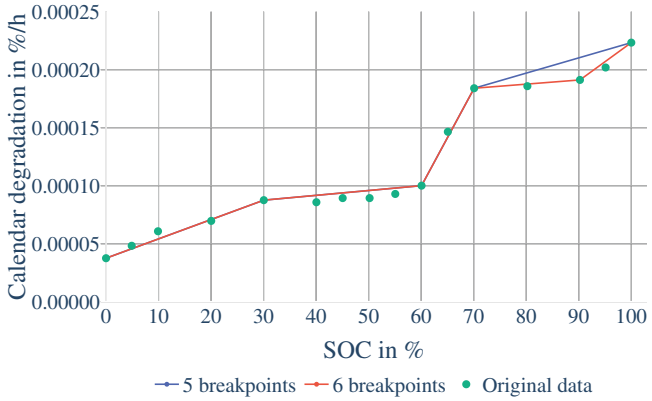

FIGURE 2 Piecewise linear approximation of calendar aging. The red line is with a sixth breakpoint at 90% SOC.

Next, we consider all three degradation mechanisms. Table 4 shows that the relative error for each component is between 1.6% and 6.6% only.

Figure 1, shows the quadratic and piecewise linear curve fits for the five original data points, and the model output data. As the quadratic curve fit is very bad for high SOC levels, we use the piecewise linear function to find the relative error for Q^{CD} of 3.24%.

Considering Q^{CAL} with 16 data measurement points (in green) in Figure 2,[1] we get a relative error of 1.62% for a piecewise linear fit with four segments (five breakpoints). Adding a sixth breakpoint at 90% SOC, improves accuracy but at the expense of an increase in solution time from 2 min to over an hour. Considering scalability, we disregard this option. The total relative error is 3.32% only. For a model run disregarding degradation, the left column in Figure 3 shows the ex post calculated degradation costs. In this case, the battery cycles to the full extent for every price arbitrage opportunity, even the smallest.

TABLE 4 Relative model degradation errors.

Degradation mechanism	Relative error [%]
Q^{CD}	3.24
Q^{SOC}	6.57
Q^{CAL}	1.62
Combined degradation	3.32

Note: Relative errors are not additive; the combined relative error is 3.32% only.

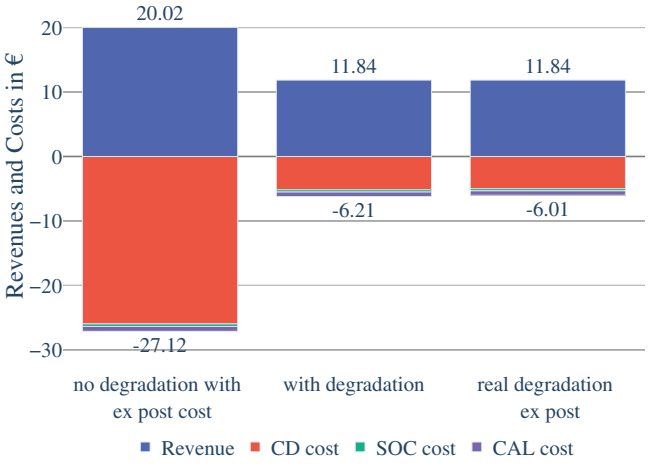

FIGURE 3 Revenues and degradation cost calculation.

In this 2-day planning horizon, the disregarded degradation costs of €27 are significantly higher than the revenues obtained, €20. When degradation is considered, revenues are about 40% lower, but degradation reduces by more than 75%. Consequently, a €7 loss turns into a €6 profit. Furthermore, in agreement with literature on grid-connected batteries, CD degradation (the red areas in the columns) is the primary degradation mechanism. The following section analyzes the impact of the individual degradation mechanisms on the SOC profile of the battery.

5.3 | Effect on SOC of degradation mechanisms

Figure 4 shows the SOC over 2 days, with and without the different degradation mechanisms considered. First, we consider *no degradation* and calendar aging *CAL*, then the cycle degradation mechanisms, before considering all three. For reference, the hourly spot price is indicated by the dashed, blue line. *No degradation* and *CAL* have almost the same SOC profile characterized as very volatile (*spiky*) cycles that exploit every price

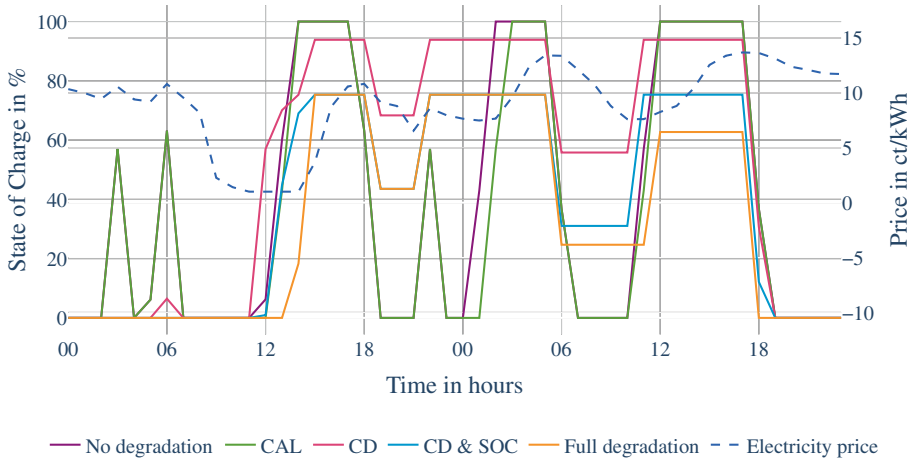

FIGURE 4 SOC comparison for different degradation mechanisms considered in the model.

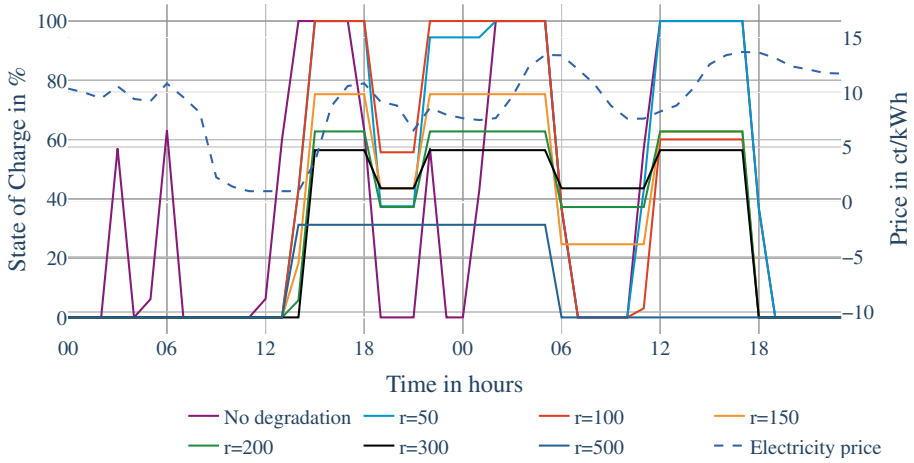

FIGURE 5 SOC for no or all three degradation mechanisms for varying battery replacement cost.

difference. Due to the overlap, *no degradation* is more clearly visible in Figure 5. This results in six cycles, three of which have a 100% CD depth that causes high battery degradation. At 00:00 on the second day, *CAL* charges with a 1-h delay compared to *no degradation*. Thereby, the battery charges at a slightly higher price, but avoids 1 h in 100% SOC, and thus some calendar aging.

In contrast with the two cases discussed so far, in hours five-six of the first day for CD, there is one, small, 10% cycle instead of a 60% cycle. This is due to the small price difference in the charge and discharge hours, which reduces profitability of larger discharges because of the discharge degradation costs. The charging in the early afternoon is more gradual, and not completely full at 93%. In the first evening, there is a much lower discharge at 18:00 of 25% only, and at midnight we see no discharge at all. The next morning at 6:00, there is a smaller discharge again, but at 18:00 there is a full discharge. The battery charged almost for free at 12:00 of the first day and now discharges for more than 13 ct/kWh. A full battery discharge is typically disallowed by lower and upper storage limits in optimization models, but here we show the benefit of directly trading off degradation costs and revenues.

In addition, consider full cycle degradation consisting of both Q^{CD} and Q^{SOC}. In this scenario, the cycle at 05:00 to 06:00 does not happen at all. Once charging starts at noon, there is a lower average SOC in the next periods. Until 18:00 the SOC is 75% (the blue and yellow lines overlap), and we see a deeper discharge at 18:00. The deeper discharge brings the average SOC during cycling closer to 50%, which is beneficial from a degradation perspective.

Finally, we observe the combination of all three mechanisms in *full degradation* line. The first day, the SOC profile is similar to that of *CD and SOC*. However, the calendar aging punishes high SOC levels, which induce the battery to charge 2 h later. This becomes more pronounced starting at 06:00 on the second day as a deeper discharge occurs (the yellow line dives below the blue line). This has two effects: calendar aging is reduced due to lower SOC levels, and Q^{SOC} is reduced (to zero) because the cycle goes from SOC 75% to SOC 25% (50% on average). In contrast, during the last charge-discharge

TABLE 5 Battery replacement costs sensitivity results (annualized by multiplying model results with 182).

KPI	Unit	$r = 50$	$r = 100$	$r = 150$	$r = 200$	$r = 300$	$r = 500$
Total charge throughput	[kWh]	249.38	194.13	137.87	108.07	78.08	29.69
Max SOC	[%]	100.00	100.00	75.32	62.75	56.44	31.25
Average SOC	[%]	42.71	37.72	32.86	30.64	29.33	10.42
Max CD	[%]	60.00	60.00	59.58	59.61	53.62	29.69
Annualized CD degradation	[%]	18.69	12.13	6.27	4.02	2.70	0.74
Annualized SOC degradation	[%]	0.29	0.75	0.44	0.29	0.34	0.27
Annualized CAL degradation	[%]	1.00	0.86	0.84	0.70	0.62	0.48
Annualized revenue	[€]	3415.63	2952.21	2161.41	1746.34	1421.5	666.72
Annualized degradation cost	[€]	999.17	1373.29	1132.51	1001.98	1098.08	742.15
Annualized profit	[€]	2416.46	1578.92	1028.9	744.35	323.42	−75.43
Pay-back period	[years]	2.1	6.3	14.6	26.9	92.8	N.A.

TABLE 6 Sets.

Set	Description
$h \in H$	Hours
$j \in J$	Battery segments
$i, m \in I$	Calendar aging breakpoints

TABLE 7 Variables.

Var.	Description
A_h^{CYC}	Auxiliary, deviation from 50% SOC
A_h^{ST}	Auxiliary, SOC at cycle start
B_h^{C}	Binary, charge mode active
$B_{i,h}^{\mathrm{CAL}}$	Binary, SOS2 variable
B_h^{D}	Binary, discharge mode active
B_h^{END}	Binary, end of a cycle
B_h^{S}	Binary, steady-state mode active
B_h^{ST}	Binary, start of a cycle
$C_{j,h}$	Battery charge
$D_{j,h}$	Battery discharge
K_h	Cost of battery degradation
N	Number of segments
Q_h^{CAL}	Calendar aging based capacity loss [%]
Q_h^{CD}	Cycle depth based capacity loss [%]
Q_h^{SOC}	Average cycle SOC-based capacity loss [%]
$S_{j,h}$	Storage level
SOC_h	State of charge
$Z_{h,i}$	SOS2 weight factor

cycle, calendar aging causes a later charge hour, a lower SOC level and lower degradation in the period 11:00 to 17:00; however, this gain is partially offset as the discharge to 0 cannot be symmetrically around 50%, thereby causing a higher Q^{SOC}.

Overall, the impact of battery degradation on optimal charging and discharging is pronounced. Considering CD-based degradation alone may result in long-lasting high resting SOC levels, as well as cycles in the higher and lower SOC spectrum, which may accelerate calendar aging. Thus it is advisable to consider multiple mechanisms.

5.4 | Sensitivity on battery replacement cost

Figure 5 and Table 5 present a range of battery replacement costs. The range from 50 to 500 €/kWh captures uncertainty in battery price forecasts[41] as well as (installation) cost differences for different battery pack sizes (note that *No degradation* corresponds with $r = 0$).

Generally, the maximum SOC level decreases and cycle amplitudes become smaller with rising replacement cost r, due to higher calendar aging costs and disproportionally high discharge costs for deep cycles. For $r = 500$ the highest SOC level is 31%, whereas for $r = 50$ and $r = 100$ it is 100%.

If batteries would become significantly cheaper, for instance, $r = 100$, or even $r = 50$, the annualized CD degradation could become very high with respective values 12.1% and 18.7%. As the profit values show, these high degradation values are more than offset by the added revenues from trading. This clearly shows the advantage of trading off degradation costs explicitly in the optimization rather than imposing hard bounds on SOC or CD. If replacement costs are lower, we can benefit more often

TABLE 8 Parameters.

Par.	Description
a^{CD}	Capacity loss for a 100% cycle
c^{MAX}	Maximum charge rate
d^{MAX}	Maximum discharge rate
e^{RAT}	Rated energy of the battery
f	Fitting parameter for average SOC stress
m	Fatigue strength exponent
o_i^{CAL}	Calendar aging mechanism breakpoint
o_j^{CD}	CD mechanism breakpoint
p_h	Electricity price (hourly)
r	Replacement cost of the battery [€/kWh]
v^C	Charging efficiency
v^D	Discharging efficiency
y_i	Calendar aging breakpoint aging value

from smaller price variations and with larger volumes from larger price deviations.

Note that for $r = 500$ there is an operating loss, but this loss would have been significantly larger if no trades had occurred. The pay-back period indications provide evidence that large-scale battery use for intra-day price arbitrage should be (close to) commercially viable. Considering future battery cost reductions, our sensitivity analysis shows that cheaper batteries lead to *spikier* charge-discharge cycles. Increasing price volatility has the same effect as lower battery costs. More frequent and larger price differences will more quickly offset degradation costs, and therefore also result in *spikier* charge-discharge cycles.

5.5 | Model runtime

The model takes 5 min 46 s to solve with $r = 150$ and considering all three degradation mechanisms. Because we wish to implement the degradation formulations in larger models, this may not be scalable. Table 5 shows that the contribution of each mechanism to the total battery degradation is very different. When the battery is very actively used, with many, and deep, cycles, $r = 50$, CD degradation accounts for 93.5% of the total degradation, Q^{CAL} 5% and Q^{SOC} 1.5% only. For the moderate, realistic $r = 150$ these values change to Q^{CD} 83.1%, Q^{CAL} 11.1% and Q^{SOC} 5.8%. Given that Q^{CD} has the most impact, we execute two additional runs, one without Q^{SOC} and one without Q^{CAL}, to assess the runtime influence of each mechanism. Combination Q^{CD}-Q^{SOC} solves in 17 s, while Q^{CD}-Q^{CAL} solves in just under a second. We conclude that Q^{SOC} has the least impact on the model accuracy but by far the biggest impact on the run time. To maintain scalability, one may remove the Q^{SOC} degradation from the optimization with little impact on model accuracy for larger systems, longer planning horizons, and in stochastic models.

6 | CONCLUSION

In this paper, we develop scalable, accurate formulations for battery degradation to allow better tradeoffs in smart grid and other technoeconomic electricity dispatch models. These formulations consider CD, average cycle SOC, and SOC-based calendar aging. We present and discuss how different degradation measures affect optimal battery operation, generally resulting in less deep charge-discharge cycles and moderated SOC levels. In many models, these damage-reducing effects are commonly enforced by merely imposing hard lower and upper bounds on SOC levels, but we emphasize this unnecessarily reduces the potential benefit from price arbitrage opportunities when price variations are very large. In a stylized, realistic setting we demonstrate profitability, and estimate a degradation model accuracy of within 3.32%. This estimate is based on linearly interpolated measurement data; real battery tests could further validate functional forms and parameter values. Two aspects are not considered in our formulation are ambient and battery cell temperature, and very high charge rates, opening up for future work. In addition, it would be interesting to apply the degradation models considering demand and generation assets in a smart grid setting.

NOMENCLATURE

C-rate	current rate
CD	cycle depth
DOD	depth of discharge
EV	electric vehicle
LFP	lithium iron phosphate
NMC	nickel manganese cobalt
SOC	state of charge
SEI	solid-electrolyte interphase

ACKNOWLEDGMENTS

We thank four anonymous reviewers for their constructive feedback.

CONFLICT OF INTEREST STATEMENT

The authors delcare no conflict of interest.

DATA AVAILABILITY STATEMENT

The data that support the findings of this study are openly available in Zenodo at https://zenodo.org/doi/10.5281/zenodo.10255080.

ORCID

Ruud Egging-Bratseth https://orcid.org/0000-0002-5061-636X

ENDNOTE

[1] The figure shows that for low and high SOC levels, capacity degradation is higher compared to levels in between. Capacity degradation is linked to the anode potential at specific SOC levels, caused by the correlation of anode potential to the loss of cyclable lithium (c.f. Keil et al[7,11]). High capacity degradation occurs during the lowest anode potential, from around 60% SOC and up for NMC cells. Degradation is more moderate in SOC range about 30% to 60% for medium anode potentials. Below 30% SOC, the anode potential is highest, and therefore capacity degradation lowest.

REFERENCES

1. Lüth A, Zepter JM, del Granado PC, Egging R. Local electricity market designs for peer-to-peer trading: the role of battery flexibility. *Appl Energy*. 2018;229:1233-1243.
2. Qiu Z, Zhang W, Lu S, et al. Charging rate based battery energy storage system model in wind farm and battery storage cooperation bidding problem. *CSEE J Power Energy Syst*. 2022;8:659-668.
3. Datta U, Kalam A, Shi J. A review of key functionalities of battery energy storage system in renewable energy integrated power systems. *Energy Storage*. 2021;3(5):e224. doi:10.1002/est2.224
4. Xiong R, Pan Y, Shen W, Li H, Sun F. Lithium-ion battery aging mechanisms and diagnosis method for automotive applications: recent advances and perspectives. *Renew Sustain Energy Rev*. 2020;131:110048. doi:10.1016/j.rser.2020.110048
5. Han X, Lu L, Zheng Y, et al. A review on the key issues of the lithium ion battery degradation among the whole life cycle. *eTransportation*. 2019;1:100005. doi:10.1016/j.etran.2019.100005
6. Thompson AW. Economic implications of lithium ion battery degradation for vehicle-to-grid (V2X) services. *J Power Sources*. 2018;396:691-709. doi:10.1016/j.jpowsour.2018.06.053
7. Keil P, Schuster SF, Wilhelm J, et al. Calendar aging of lithium-ion batteries. *J Electrochem Soc*. 2016;163(9):A1872-A1880. doi:10.1149/2.0411609jes
8. Ahmadian A, Sedghi M, Elkamel A, Fowler M, Aliakbar Golkar M. Plug-in electric vehicle batteries degradation modeling for smart grid studies: review, assessment and conceptual framework. *Renew Sustain Energy Rev*. 2018;81:2609-2624. doi:10.1016/j.rser.2017.06.067
9. Xu B, Zhao J, Zheng T, Litvinov E, Kirschen DS. Factoring the cycle aging cost of batteries participating in electricity markets. *IEEE Trans Power Syst*. 2018;33(2):2248-2259.
10. Zhou C, Qian K, Allan M, Zhou W. Modeling of the cost of EV battery wear due to V2G application in power systems. *IEEE Trans Energy Convers*. 2011;26(4):1041-1050.
11. Edge JS, O'Kane S, Prosser R, et al. Lithium ion battery degradation: what you need to know. *Phys Chem Chem Phys*. 2021;23:8200-8221. doi:10.1039/D1CP00359C
12. Chengquan J, Wang P, Goel L, Xu Y. A two-layer energy management system for microgrids with hybrid energy storage considering degradation costs. *IEEE Trans Smart Grid*. 2018;9(6):6047-6057.
13. Guenther C, Schott B, Hennings W, Waldowski P, Danzer MA. Model-based investigation of electric vehicle battery aging by means of vehicle-to-grid scenario simulations. *J Power Sources*. 2013;239:604-610. doi:10.1016/j.jpowsour.2013.02.041
14. Wang J, Liu P, Hicks-Garner J, et al. Cycle-life model for graphite-$LiFePO_4$ cells. *J Power Sources*. 2011;196(8):3942-3948. doi:10.1016/j.jpowsour.2010.11.134
15. Wang D, Coignard J, Zeng T, Zhang C, Saxena S. Quantifying electric vehicle battery degradation from driving vs. vehicle-to-grid services. *J Power Sources*. 2016;332:193-203. doi:10.1016/j.jpowsour.2016.09.116
16. Laresgoiti I, Käbitz S, Ecker M, Sauer D. Modeling mechanical degradation in lithium ion batteries during cycling: solid electrolyte interphase fracture. *J Power Sources*. 2015;12(300):112-122.
17. Baghdadi I, Briat O, Delétage JY, Gyan P, Vinassa JM. Lithium battery aging model based on Dakin's degradation approach. *J Power Sources*. 2016;325:273-285. doi:10.1016/j.jpowsour.2016.06.036
18. Wu W, Wu W, Qiu X, Wang S. Low-temperature reversible capacity loss and aging mechanism in lithium-ion batteries for different discharge profiles. *Int J Energy Res*. 2019;43(1):243-253. doi:10.1002/er.4257
19. Gao Y, Jiang J, Zhang C, Zhang W, Ma Z, Jiang Y. Lithium-ion battery aging mechanisms and life model under different charging stresses. *J Power Sources*. 2017;356:103-114. doi:10.1016/j.jpowsour.2017.04.084
20. Bhagavathy SM, Budnitz H, Schwanen T, McCulloch M. Impact of charging rates on electric vehicle battery life. *Findings*. 2021;21459. https://doi.org/10.32866/001c.21459.
21. Olmos J, Gandiaga I, de Ibarra AS, Larrea X, Nieva T, Aizpuru I. Modelling the cycling degradation of Li-ion batteries: chemistry influenced stress factors. *J Energy Storage*. 2021;40:102765. doi:10.1016/j.est.2021.102765
22. Reniers JM, Mulder G, Ober-Blöbaum S, Howey DA. Improving optimal control of grid-connected lithium-ion batteries through more accurate battery and degradation modelling. *J Power Sources*. 2018;379:91-102. doi:10.1016/j.jpowsour.2018.01.004
23. Yusuf J, Ula S. A comprehensive optimization solution for buildings with distributed energy resources and V2G operation in smart grid applications. Paper presented at: 2020 IEEE Power Energy Society Innovative Smart Grid Technologies Conference. 2020.
24. Shakeri M, Shayestegan M, Abunima H, et al. An intelligent system architecture in home energy management systems (HEMS) for efficient demand response in smart grid. *Energy Build*. 2017;138:154-164.
25. Reniers JM, Mulder G, Howey DA. Unlocking extra value from grid batteries using advanced models. *J Power Sources*. 2021;487:229355. doi:10.1016/j.jpowsour.2020.229355
26. Smith AJ, Svens P, Varini M, Lindbergh G, Lindström RW. Expanded in situ aging indicators for lithium-ion batteries with a blended NMC-LMO electrode cycled at sub-ambient temperature. *J Electrochem Soc*. 2021;168(11):110530. doi:10.1149/1945-7111/ac2d17
27. Naumann M, Spingler FB, Jossen A. Analysis and modeling of cycle aging of a commercial $LiFePO_4$/graphite cell. *J Power Sources*. 2020;451:227666. doi:10.1016/j.jpowsour.2019.227666

28. Sarasketa-Zabala E, Gandiaga I, Rodriguez-Martinez LM, Villarreal I. Calendar ageing analysis of a $LiFePO_4$/graphite cell with dynamic model validations: towards realistic lifetime predictions. *J Power Sources*. 2014;272:45-57. doi:10.1016/j.jpowsour.2014.08.051
29. de Hoog J, Timmermans JM, Ioan-Stroe D, et al. Combined cycling and calendar capacity fade modeling of a nickel-manganese-cobalt oxide cell with real-life profile validation. *Appl Energy*. 2017;200:47-61. doi:10.1016/j.apenergy.2017.05.018
30. Loew S, Anand A, Szabo A. Economic model predictive control of Li-ion battery cyclic aging via online rainflow-analysis. *Energy Storage*. 2021;3(3):e228. doi:10.1002/est2.228
31. Bjarghov S, Kalantar-Neyestanaki M, Cherkaoui R, Farahmand H. Battery degradation-aware congestion management in local flexibility markets. Paper presented at: 2021 IEEE PowerTech IEEE. 2021. doi:10.1109/PowerTech46648.2021.9494829
32. Zhang L, Yu Y, Li B, et al. Improved cycle aging cost model for battery energy storage systems considering more accurate battery life degradation. *IEEE Access*. 2022;10:297-307.
33. Shi Y, Xu B, Tan Y, Kirschen D, Zhang B. Optimal battery control under cycle aging mechanisms in pay for performance settings. *IEEE Trans. Automat. Control*. 2019;64(6):2324-2339.
34. Bansal RK, You P, Gayme DF, Mallada E. Storage degradation aware economic dispatch. Paper presented at: 2021 American Control Conference. 2021.
35. Shi Y, Xu B, Tan Y, Zhang B. A convex cycle-based degradation model for battery energy storage planning and operation. Paper presented at: Annual American Control Conference. 2018.
36. Upadhya S, Wagner MJ. A dispatch optimization model for hybrid renewable and battery systems incorporating a battery degradation model. *J Energy Resour Technol*. 2021;144:070907. doi:10.1115/1.4052983
37. Schade C, Egging-Bratseth R. Battery degradation: impact on economic dispatch—data documentation. *Zenodo*. 2023. doi:10.5281/zenodo.10255080
38. Bundesnetzagentur. Marktdaten. 2019 https://www.smard.de/home/downloadcenter
39. Electricity Price. 2019. https://strom-report.de/strompreise/#strompreiszusammensetzung
40. Imamoto A, Tang B. A recursive descent algorithm for finding the optimal minimax piecewise linear approximation of convex functions. *Lect Notes Eng Comput Sci*. 2008;10:2173.
41. Mauler L, Duffner F, Zeier WG, Leker J. Battery cost forecasting: a review of methods and results with an outlook to 2050. *Energ Environ Sci*. 2021;14:4712-4739.

How to cite this article: Schade C, Egging-Bratseth R. Battery degradation: Impact on economic dispatch. *Energy Storage*. 2024;6(2):e588. doi:10.1002/est2.588